THE JOURNAL OF PHYSICAL CHEMISTRY B

Article

pubs.acs.org/JPCB

Effect of Hydrophilicity or Hydrophobicity of Polyelectrolyte on the Interaction between Polyelectrolyte and Surfactants: Molecular Dynamics Simulations

Zhenhai Liu,[†] Yazhuo Shang,*[,†] Jian Feng,[‡] Changjun Peng,[†] Honglai Liu,[†] and Ying Hu[†]

[†]State Key Laboratory of Chemical and Engineering and Department of Chemistry, East China University of Science and Technology, Shanghai 200237, China

[‡]Department of Chemistry and Life Science, Chuzhou University, Anhui 239012, China

Supporting Information

ABSTRACT: The effect of hydrophilicity or hydrophobicity of polyelectrolyte on the interaction between polyelectrolyte and oppositely charged surfactants was investigated by using coarse-grained molecular dynamics simulations. The aggregation of surfactants on the hydrophilic polyelectrolyte is significantly different from that on the hydrophobic polyelectrolyte. The complexes evolve from the "bottle brush", through the "necklace", then to the micelle. However, the rod-like micelle, in which polyelectrolyte wraps around the micelle surface, only appears in the hydrophilic polyelectrolyte system. For the hydrophobic polyelectrolyte system, the spherical micelle is formed, and the polyelectrolyte penetrates into the hydrophobic core of complexes. The hydrophobic nature of the surfactant tails induces the surfactant's tendency to depart from the hydrophilic polyelectrolyte and point toward the bulk phase, but it is apt to combine with the hydrophobic polyelectrolyte, leading to a parallel configuration between the surfactants and the polyelectrolyte. When the charge ratio (Z) of surfactant to polylelectrolyte is lower, the polyelectrolyte shows extended structure, and with the increase of Z, the polyelectrolyte collapse undergoes either a continuous or an abrupt change depending on if it is a hydrophobic or hydrophilic polyelectrolyte. At higher charge density of the hydrophilic polyelectrolyte, there is a synergistic effect of the electrostatic interaction between surfactant and polyelectrolyte, with the hydrophobic interaction among the adsorbed surfactants. For the hydrophobic polyelectrolyte system, no synergistic effect is observed.

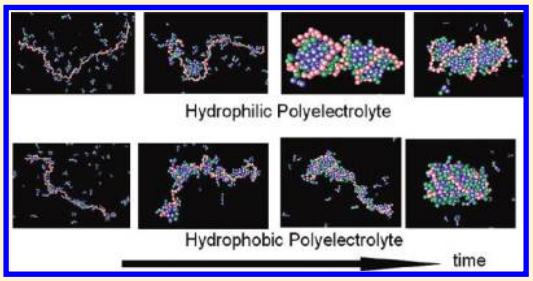

1. INTRODUCTION

Interactions between polyelectrolytes and surfactants bearing opposite charges in aqueous solutions have attracted significant attention because of their relatively complex behaviors and potential applications in many areas, such as rheological control, drug delivery, protein separation, functional materials preparation, detergency and pharmaceutical formulations, etc.[1−6] A number of research groups have devoted their attention to the complex formation, phase behavior, thermodynamics, and morphology of the complexes in these systems. The strong electrostatic attraction and the hydrophobic interaction between polyelectrolytes and oppositely charged surfactants have been confirmed by the occurrence of binding of surfactants on polyelectrolyte chains at a surfactant concentration several orders of magnitude lower than the critical micelle concentration (CMC) of the free surfactants. The binding behavior including the binding process and the complex morphologies is affected by many factors related to the structures,[7] chain flexibility and charge density of polyelectrolyte,[8−11] the nature of surfactant pH,[12,13] the ionic strength of media,[14−19] and so on. The morphologies of the complexes vary with the concentration of the surfactant. Most of the studies focus on the system with lower surfactant concentration to avoid the precipitation of ordered nanostructure usually appearing in the polyelectrolyte/surfactant mixed systems when the surfactant concentration is higher. The necklace-like structure, where some beadlike structures formed by surfactants disperse on polyelectrolyte chains randomly, is usually observed at the lower surfactant concentration.[20,21] The condensed toroidal aggregates derived from the spiral wrap of polyelectrolyte around cylindrical surfactant micelle surface are also proposed. The transformation between the two kinds of complexes by adjusting the experimental conditions is explored by Viet and Lynn.[22] Nause et al. studied the variation of complex morphology with charge ratio for the mixed system of CTAC/PSS by SANS and SAXS, and the necklace-like structure and cylindrical surfactant micelle are both observed.[23] However, the experimental study on the properties of the polyelectrolyte−surfactant complex in the low surfactant concentration region is far from satisfactory. Although the combination of static and dynamic light scattering, TEM, and SEM techniques can provide related information, such as the

Received: December 15, 2011
Revised: April 14, 2012
Published: April 23, 2012

shape, molecular mass, radius of gyration, and hydrodynamic radius of the complexes, the detailed complex process and the subtle internal structure of complex cannot be depicted directly by using these instruments. It is difficult to obtain reliable and convictive information on the interaction of polyelectrolyte and surfactant by experimental methods easily.[4] A more effective substitute is expected.

Recently, theoretical studies on the interaction between polyelectrolyte and surfactant prevail. Shirahama et al. modeled polyelectrolyte as a rigid chain and used the Ising model to estimate the parameter.[24] Gurovitch and Sens proposed an idealized model within the framework of the self-consistent field theory for the adsorption of a weakly charged polyelectrolyte chain onto an oppositely charged colloidal particle.[25] The thermodynamic approach and scaling approach were used by Diamant and Andelman to explore the interaction between a flexible polymer in a good solvent and surfactants.[26] The self-consistent field lattice model was adopted to predict the formation of complexes by assuming that the complex has spherical symmetry structure.[27] Kuhn and Diehl proposed a simple model to describe conformational behavior of flexible polyelectrolytes in the presence of monovalent cationic surfactants and found a discrete conformational transition between an elongated coil and a compact globule.[28] In some thermodynamic models, the surfactant micelles are modeled as a large charged hard sphere to simplify the model; this means that the degree of freedom of the surfactant chain is integrated.[29−31] Mateescu et al. simplified the charged micelles as macroions when they examined the effect of the amount of charges carried by micelles and polyelectrolyte on the interaction between strong polyelectrolyte and oppositely charged micelles.[29] In other models, the structure of the polyelectrolyte chain was simplified. For example, the DNA chain can be approximately modeled as a uniform infinite cylinder with specified charge density, which could ignore the intrachain degree of freedom of polyelectrolyte.[32] On the basis of these models, the expression of the free energy of the system can be obtained. It is obvious that the free energy reaches a minimum when the system is in equilibrium, and so the equilibrium structure of the complex can be determined. According to the thermodynamic equilibrium condition of a system, the chemical potential of surfactants in a complex should equal that of the free surfactant in bulk solution when the system is in equilibrium, and therefore the chemical potential of the surfactant that forms the complex can also be obtained.[33] However, the methods mentioned above are often based on the drastic assumptions of the complex structure or its symmetry. Just as Ferber and Löwen pointed out, one "...cannot predict the complex structure or its symmetry as far as it enters the theory as an input", so these models inevitably have some deficiencies.[34] In addition, the Debye−Hückel theory was often used to model the polyelectrolyte−surfactant system for the long-range electrostatic interactions in the electrolyte solution, which does not properly handle the Manning condensation phenomena occurring under certain conditions due to the strong electrostatic correlation.[35,36] The study on the interaction between polyelectrolyte and surfactant still remains a significant challenge.

Molecular simulation for the morphologies of the complexes formed by polyelectrolytes and oppositely charged surfactants has been carried out to provide a better understanding of structures on the molecular scale, as well as larger scale morphological structures and chemical functionalities of complexes. Excellent work using a variety of different simulation techniques has been reported.[34,37−42] This approach is much more realistic from a practical perspective as compared to previous approaches. The most important advantage of the molecular simulation is that there is no prior assumption on the structure and symmetry of the complex, so the real kinetics of complex formation, which is very difficult to observe in experiment, can be studied. However, in most of these studies, surfactant micelles are usually treated as a hard sphere carrying given charges[37−40] for the sake of deceasing simulation time, but it cannot reveal the inner structure of the complex. Furthermore, the charged hard sphere cannot mimic the real micelle especially when the size and the shape of the micelle are changed due to the variation of surfactant number in the micelle, although the hard sphere adsorbed on the polyelectrolyte chain can get close to each other. In Groot's work, they studied the interaction of the surfactant and the polyelectrolyte by treating surfactant as a flexible molecule consisting of a hydrophilic headgroup and a hydrophobic tail chain, and found that without surfactant the polyelectrolyte chain acts as a rigid one, while the polyelectrolyte chain will wrap on the micelle after the surfactant is added.[41] Ferber and Löwen studied the complex structure formed by polyelectrolyte and surfactants with different hydrophobic and electrostatic interaction by using the Monte Carlo (MC) simulation.[34] They also treat the surfactant as a chain molecule consisting of a single charged head bead tethered to a tail with some tethering hard spheres and introduce a hydrophobic attraction between the tail beads by assuming a Lennard-Jones potential outside the hard-sphere diameter. The transition between the "bottle-brush structure" and the spherical micelle structure with changing strength of hydrophobic and electrostatic interaction has been found. In summary, for the major studies on the interaction of surfactant and polyelectrolyte reviewed above, different perspectives were proposed. However, all of the work treats the polyelectrolyte chain as a hydrophilic one without considering the fact that some polyelectrolyte chains are fairly hydrophobic.[43−46] It is obvious that the hydrophobic polyelectrolyte chain can penetrate into the micelle and participate in the formation of micelle further; therefore, the micelles cannot be treated as hard spheres. Meanwhile, treating the beads of all polyelectrolyte chains as completely hydrophilic and modeling the micelle as a hard charged sphere are absolutely unreasonable. It is worth mentioning that Groot et al. also considered the hydrophobicity of polyelectrolyte; however, the long-range electrostatic interaction has not been involved in their work.[42] By far, the study on the interaction between polyelectrolyte and surfactants considering both hydrophobic interaction and electrostatic interaction has still not been undertaken to the best of our knowledge.

In the present work, the interactions of polyelectrolyte and oppositely charged surfactants were systematically studied by using coarse-grained MD simulation. The effects of hydrophilicity or hydrophobicity of the polyelectrolyte chain and the electrostatic interaction between polyelectrolyte and surfactant were considered simultaneously. The mechanism of polyelectrolyte/surfactant complexation and the morphology of the polyelectrolyte/surfactant complex were elucidated. We expect to gain deep insight into the effects of the hydrophilicity and hydrophobicity of the polyelectrolyte chain, the concentration ratio of surfactants to polyelectrolyte, and the charge density of polyelectrolyte on the interaction of surfactants with polyelectrolyte.

2. SIMULATION DETAILS

The simulation system is composed of one polyelectrolyte chain and different numbers N_s of surfactants. Both the polyelectrolyte chain and the surfactant are modeled as a spring-bead chain. The polyelectrolyte chain includes $N_p = 100$ monomers carried with negative charges M_p. Each surfactant molecule includes one charged head bead carrying a positive charge $M_s = 1$ and $N_t = 3$ hydrophobic tail beads. The solvent is treated as a continuous medium with a permittivity ξ. Corresponding monovalent counterions of the polyelectrolyte and the surfactant are introduced to reach electroneutrality in the system. For simplicity, all particles including the segments of the polyelectrolyte and the surfactant and the counterions are assumed to have the same mass m and diameter σ.

The short-range interaction between particles i and j at r distance is modeled by the truncated shifted Lennard-Jones (LJ) potential.

$$u_{ij}^{\mathrm{LJ}}(r) = \begin{cases} 4\varepsilon\left[\left(\frac{\sigma}{r}\right)^{12} - \left(\frac{\sigma}{r}\right)^{6} - \left(\frac{\sigma}{r_c}\right)^{12} + \left(\frac{\sigma}{r_c}\right)^{6}\right] & r < r_c \\ 0 & r \geq r_c \end{cases} \quad (1)$$

where r_c is the cutoff distance. The hydrophilicity and the hydrophobicity are described by the LJ potential with different parameters.

For the hydrophilic polyelectrolyte systems, the cutoff length of all bead pairs except that of the tail−tail is taken to be $r_c = 2^{1/6}\sigma$. To model the hydrophobic surfactant tail, we introduce an attractive cutoff distance $r_c = 2.5\sigma$ for the interaction between tail beads. For hydrophobic polyelectrolyte systems, besides the tail−tail, the cutoff distances between monomers of polyelectrolyte chain and the monomer−tail are all taken to be $r_c = 2.5\sigma$ to describe the hydrophobicity of the polyelectrolyte chain.

The long-range interaction between charged beads i and j with charges z_i and z_j is modeled by the coulomb potential:

$$u_{ij}^{\mathrm{ELE}}(r) = \frac{e^2}{4\pi\xi}\frac{z_i z_j}{r} = \frac{\lambda_B z_i z_j}{r} k_B T \quad (2)$$

where e is unit charge; $\xi = \xi_0\xi_r$, where ξ_0 and ξ_r are the vacuum permittivity and the dielectric constant of the solvent, respectively; and λ_B is the Bjerrum length:

$$\lambda_B \equiv \frac{e^2}{4\pi\xi k_B T} \quad (3)$$

where k_B is the Boltzmann constant, and T is the system temperature.

The chain's connectivity is maintained by a finitely extendable nonlinear elastic (FENE) potential:

$$u_{ij}^{\mathrm{FENE}}(r) = \begin{cases} -\frac{1}{2}kR_0^2\ln\left[1 - \left(\frac{r}{R_0}\right)^2\right] & r \leq R_0 \\ \infty & r > R_0 \end{cases} \quad (4)$$

where $k = 30\varepsilon/\sigma^2$ is the spring constant, and $R_0 = 2\sigma$ is the maximum extension.

The motion of each bead in the system is governed by the stochastic Langevin equation, which accounts for the viscous force from solvent and the stochastic force from a heat-bath:

$$m\frac{\mathrm{d}^2 r_i}{\mathrm{d}t^2} = -\nabla U_i - \gamma\frac{\mathrm{d}r_i}{\mathrm{d}t} + W_i(t) \quad (5)$$

where r_i is the position of bead i, and γ is the friction coefficient. $W_i(t)$ is a random force exerting on particle j at time t, which satisfies:

$$\langle W_i(t)W_i(t')\rangle = 6k_B T\gamma\delta_{ij}\delta(t - t') \quad (6)$$

where k_B is the Boltzmann constant, and T is the absolute temperature of the system.

U_i is the interaction energy of the bead i with all of the other beads in the system:

$$U_i = \sum_{j\neq i} u_{ij}(r) = \sum_{j\neq i}\left[u_{ij}^{\mathrm{LJ}}(r) + u_{ij}^{\mathrm{ELE}}(r) + u_{ij}^{\mathrm{FENE}}(r)\right] \quad (7)$$

The electrostatic interactions are calculated using the Particle Mesh Ewald (PME) algorithm.[47]

The simulation was performed in a cubic box with a length $L = 100\sigma$ with the periodic boundary conditions in three dimensions. The simulation box is large enough to avoid the finite size effect. The integral time step was 0.005τ, where $\tau = \sigma(m/\varepsilon)^{1/2}$. The friction coefficient γ is set to $\gamma = 1.0\tau^{-1}$. The total time steps of simulation were 8×10^6 steps, in which the last 3×10^6 steps were used to obtain ensemble averages. The Bjerrum length λ_B of water at room temperature is 0.71 nm. To match the fact, we let $\lambda_B = 2\sigma$ and reduced the temperature $T = 1.0$. The charge ratio of systems was defined by $Z = N_s M_s/N_p M_p$, so the corresponding system concentration of surfactant can be calculated by $\rho_s = N_s/L^3 = ZN_p M_p/M_s L^3$. The system concentration of polyelectrolyte is $\rho_p\sigma^3 = 10^{-6}$.

3. RESULTS AND DISCUSSION

3.1. Binding of Surfactants on Polyelectrolyte. The binding of surfactants on the hydrophilic and hydrophobic polyelectrolytes was explored. The binding processes of the two systems show significant difference. Figure 1 depicts the

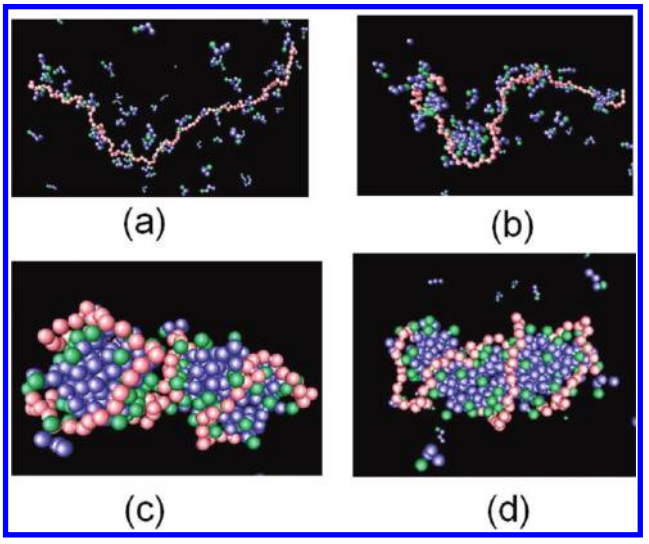

Figure 1. Snapshots of the adsorption process of surfactants on the hydrophilic polyelectrolyte. (a) Surfactants adsorb on the polyelectrolyte chain and form a "bottle-brush" structure. (b) "Bottle-brush" structure evolves into necklace structures. (c) The size of the "beads" on the polyelectrolyte gradually becomes larger. (d) The polyelectrolyte chain and surfactants form stable rod-like micelle.

dx.doi.org/10.1021/jp212089d | J. Phys. Chem. B 2012, 116, 5516−5526

adsorption panorama of the surfactants on the hydrophilic polyelectrolyte at a charge ratio of $Z = 1.5$ (the corresponding system concentration of surfactant $\rho_s\sigma^3 = 1.5 \times 10^{-4}$). From the snapshot of the adsorption process, we can see that the adsorption process can be generalized as four typical stages. In the first stage, the charged surfactant head is adsorbed on the polyelectrolyte due to the strong electrostatic interaction, and the hydrophobic tail of the surfactant is expelled away from the polyelectrolyte chain. The bottle-brush structure is formed, as shown in Figure 1a. The second stage as shown in Figure 1b can be summarized as the evolution from the bottle-brush structure into a so-called necklace structure. With the increase of the amount of the surfactant adsorbed on the polyelectrolyte, the local concentration of the surfactant around the polyelectrolyte increases, and the short-range hydrophobic interaction between surfactant hydrophobic tails promotes the aggregation of the adjacent surfactants and thus forms micelle-like "beads". Meanwhile, the electrostatic repulsion of the polyelectrolyte is shielded by the oppositely charged surfactants, which endows the flexibility of the polyelectrolyte chain, and the necklace structure is formed. In the third stage, as shown in Figure 1c, the short-range hydrophobic interaction causes the "bead" on the polyelectrolyte to adsorb the free surfactants further in the solution and form relatively larger spherical micelles, while the flexible polyelectrolyte wraps around the surface of the micelles and inevitably links the two micelles together. In the final stage, the "linker" pulls the micelles closer, and finally the two micelles fuse into one rod-like micelle, as shown in Figure 1d. The result is in agreement with experimental observations by Ilekti[48] and Nause.[23] It is worth noting that not all systems undergo the four stages, as the binding process and the final structure of the complex depend on not only the nature, the concentration of the surfactant, and polyelectrolyte, but also the mixing ratio of the surfactant to polyelectrolyte.

Figure 2 shows the adsorption structure of surfactant on a hydrophobic polyelectrolyte and the corresponding process of the formation of surfactant/polyelectrolyte complex at $Z = 1.5$. The process also can be divided into four stages, while the structure of the complex is obviously different as compared to that formed in the hydrophilic polyelectrolyte system. The typical bottle-brush structure is also observed in the first stage. The headgroup of the surfactant gets closer to the polyelectrolyte, and the tail of the surfactant tends to stick on the polymer chain too because of the coexistence of electrostatic interaction and hydrophobic interaction between surfactant and polyelectrolyte. As compared to the tail, the headgroup is relatively far from the polyelectrolyte, the reason for which will be elucidated in the next section. Subsequently, the bottle brush evolves into a necklace structure followed by the growth of the "beads", and then reaches the final state. In the final stage, the surfactant and the polyelectrolyte form a spherical micelle instead of the rod-like micelle, and the hydrophobic polyelectrolyte penetrates into the hydrophobic core rather than wraps around the surface of the micelle as compared to the system containing hydrophilic polyelectrolyte.

It is worth mentioning that Yethiraj et al. argue that there are qualitative differences between the results obtained by using molecular dynamics simulation with implicit solvent model and explicit solvent model for some polymer systems, and they have many significant works in this field.[49−52] To explore the difference between the results obtained by models of implicit and explicit solvent for the present system, two systems at $Z =$ 1.5 were studied by using molecular simulation with explicit solvent. According to Chang and Yethiraj's work, a solvent quality parameter λ is introduced in the studied systems.[51] For the hydrophilic system, we set $\lambda = 0$ for any pairs except the pairs of beads of surfactant tail ($\lambda = 1$). For the hydrophobic system, we set $\lambda = 1$ between any beads of surfactant tail, monomer (of polyelectrolyte)−bead (of surfactant tail), monomer−monomer, solvent−solvent, and $\lambda = 0$ for other pairs. The solvent molecule has the same mass and size as other beads, and the concentration $\rho_{sol}\sigma^3 = 0.01$. Other simulation details are the same as the description above. The result (snapshot was shown in Figure 3) provided an adsorption process similar to that obtained by using MD simulation with implicit solvent, and they are quantitatively consistent. For example, the rod-like micelle was formed for the hydrophilic

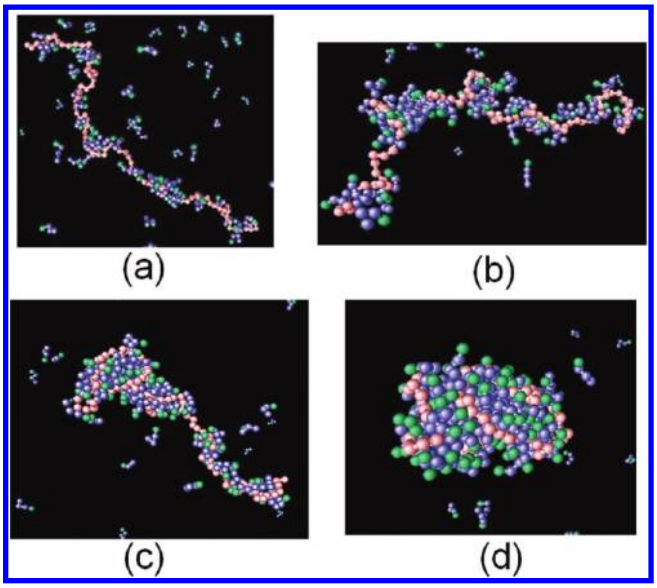

Figure 2. Snapshots of the adsorption process of surfactants on the hydrophobic polyelectrolyte. (a) Surfactants adsorb on the polyelectrolyte chain and form a "bottle-brush" structure. (b) "Bottle-brush" structure evolves into necklace structures. (c) The size of the "beads" on the polyelectrolyte gradually becomes larger. (d) The polyelectrolyte chain and surfactants form stable sphere-like micelle.

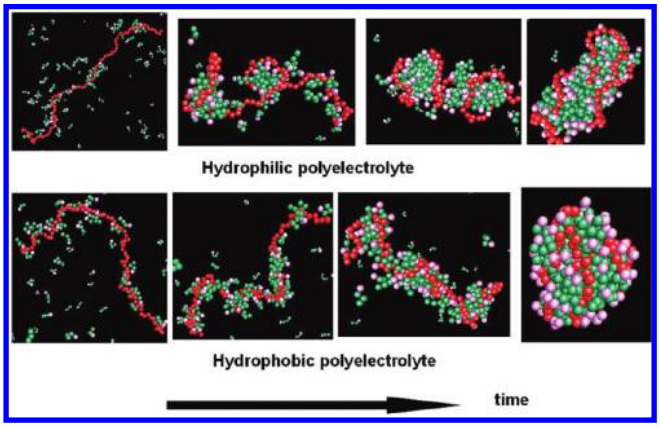

Figure 3. Snapshot of the adsorption process of surfactants on the hydrophilic and hydrophobic polyelectrolyte using MD simulation with explicit solvent at $Z = 1.5$. For clarity, solvent molecules and counterions are not shown.

dx.doi.org/10.1021/jp212089d | J. Phys. Chem. B 2012, 116, 5516−5526

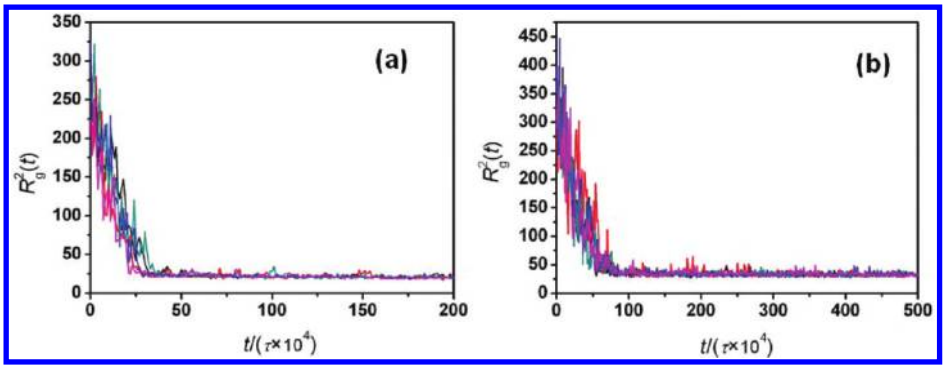

Figure 4. Five independent MD trajectories for the variation of the square radius of gyration with time at $Z = 1.5$ for the hydrophobic system (a) and hydrophilic system (b).

system; however, the spherical micelle was found in the hydrophobic system.

Chang and Yethiraj studied the dynamics of collapse of homopolymer in poor solvent using Brownian dynamics with implicit solvent and molecular dynamics simulations with explicit solvent.[49] They found that the homopolymer was trapped in local minima and occasionally jumps from one minimum in the complex landscape to another using Brownian dynamics with implicit solvent, but these phenomena were not observed when they used molecular dynamics simulations with explicit solvent. The chain size occurs in discrete jumps, and the trajectories do not reach the equilibrium. In this work, we use molecular dynamics simulations with implicit solvent, and to avoid this kind of defect mentioned above, we followed their work and chose 50 independent initial configurations for the hydrophilic system and hydrophobic system, respectively, for the simulation, and the discrete jumps of the square radius of gyration are not observed for any studied system. It is clear that all systems reach equilibrium state. Figure 4a and b provides five independent MD trajectories for the variation of the square radius of gyration with time for hydrophobic and hydrophilic polyelectrolyte systems. The square radius of gyration was defined by:

$$\langle R_g^2 \rangle = \frac{1}{N^2} \sum_{i=1}^{N} \sum_{j=i}^{N} \langle (R_j - R_i)^2 \rangle \tag{8}$$

Furthermore, the normalized mean square radius of gyration ($C_{RG}(t)$) was investigated.

$$C_{RG}(t) \equiv \frac{\langle R_g^2(t) \rangle}{\langle R_g^2(0) \rangle} \tag{9}$$

Figure 5 depicts the variation of $C_{RG}(t)$ with reduced time in the MD simulations for hydrophobic and hydrophilic system. As can be seen from Figure 5, the relaxation time of the hydrophobic system is shorter than that of the hydrophilic system. We found that the initial collapse process could be well fitted by the stretched exponential function:

$$C_{RG}(t) = \exp(-(t/\iota)^{\beta}) \tag{10}$$

where τ and β are fit parameters. We obtained $\beta = 1.22$ for the hydrophilic system and $\beta = 1.14$ for the hydrophobic system. It is clear that the relaxation time of the hydrophobic system is shorter than that of the hydrophilic system, and the hydrophobic polyelectrolyte is easier to collapse. As a last test, we chose randomly a spherically collapsed structure taken

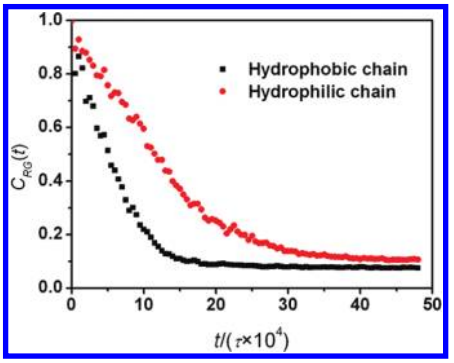

Figure 5. Variation of $C_{RG}(t)$ with reduced time in the MD simulations at $Z = 1.5$ for the hydrophobic and hydrophilic system.

from hydrophobic complexes as the initial configuration at $Z = 1.5$ and performed the simulation turning off the hydrophobicity. The result shows that the spherical complex turns into a cylindrical shape. It reconfirms that the system is indeed in equilibrium (the snapshot of the transformation is provided in the Supporting Information).

3.2. Morphology of Surfactant/Polyelectrolyte Complex. The morphology of the surfactant/polyelectrolyte complex can be quantitatively characterized by the radius distribution function (RDF) of the surfactant headgroup around the polyelectrolyte chain. The equilibrium structures of the complexes vary with the change of charge ratio Z. Figure 6 shows the RDF of the surfactant headgroup to the hydrophilic polyelectrolyte chain at $Z = 0.2$, 0.3, 0.5, 0.75, 1.0, 1.25, and 1.5 (the corresponding system concentrations of

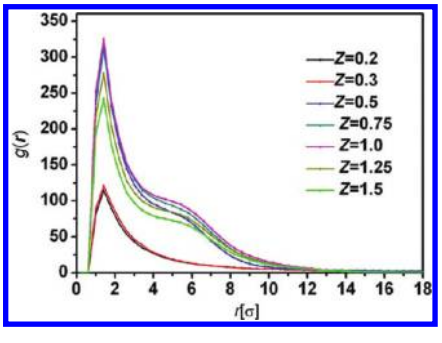

Figure 6. Radial distribution function of the headgroup of surfactants around the monomers of the hydrophilic polyelectrolyte with different charge ratio Z. At $Z = 0.2$ and 0.3, there is only one peak at $r = 1.4\sigma$. At $Z = 0.5-1.5$, there is another small peak that appears at $r = 5.5\sigma$.

dx.doi.org/10.1021/jp212089d | J. Phys. Chem. B 2012, 116, 5516–5526

surfactant are $\rho_s\sigma^3 = 2 \times 10^{-5}$, 3×10^{-5}, 5×10^{-5}, 7.5×10^{-5}, 1×10^{-4}, 1.25×10^{-4}, and 1.5×10^{-4}), respectively. From Figure 6, we can see that a single peak appears at $r = 1.4\sigma$ when $Z = 0.2$ and 0.3. Combined with the simulation snapshot and the given diameter (σ) of the particles in the simulation box, it is considered that the peak is derived from the formation of complex with bottle-brush structure, in which surfactant adsorbs on the polyelectrolyte chain. Obviously, there are a lot of unoccupied adsorption sites on the polyelectrolyte when the surfactant concentration is lower and the distance between the surfactants adsorbed on the polyelectrolyte chain is larger. Correspondingly, the larger distance makes the short-range hydrophobic interaction among the surfactant tails less obvious; therefore, the electrostatic repulsive effect of polyelectrolyte itself prevails, and the polyelectrolyte presents an extended state. As the concentration of the surfactant increases up to $Z = 0.5$, an extra shoulder peak appears at $r = 5.5\sigma$ except for that at $r = 1.4\sigma$. The shoulder peak embodies the formation of the micelle around the polymer. The short-range hydrophobic interaction among surfactants promotes the formation of the micelle around the polyelectrolyte chain at relatively low surfactant concentration, so some of the surfactant headgroups do not locate on or around the polyelectrolyte chain but distribute at about $r = 5.5\sigma$. The results indicate that the critical aggregate concentration (CAC), that is, the surfactant concentration C_{surf} of forming aggregates, is reached at $Z = 0.5$. Correspondingly, the complex evolves from bottle-brush to necklace structure.

The adsorption morphologies of surfactant on hydrophilic and hydrophobic polyelectrolytes are different. To detect the difference, the RDFs for the surfactant headgroup and the last bead of the surfactant tail with respect to the polyelectrolyte chain at $Z = 0.3$ were further studied separately. As shown in Figure 7, the r value at the peak for headgroup is smaller than

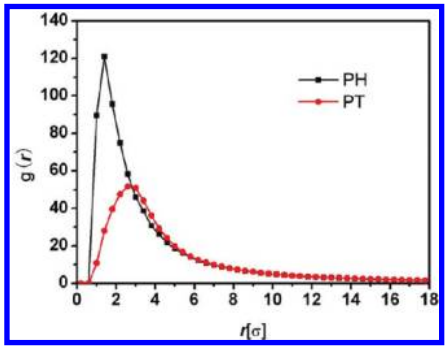

Figure 7. Radial distribution function of the headgroup of surfactants and the last bead of the surfactant tail around the monomers of the hydrophilic polyelectrolyte at charge ratio $Z = 0.3$.

that for the tail when the polyelectrolyte is hydrophilic, which suggests that the surfactant head adsorbs on the polyelectrolyte chain and the tail points to the solvent. As for the hydrophobic polyelectrolyte shown in Figure 8, the opposite result is observed; that is, the tail of the surfactant is a little closer to the polyelectrolyte chain than is the headgroup. To a certain extent, the difference between the RDF peaks of the surfactant headgroup and the tail can reflect the configuration of the surfactants with respect to the polyelectrolyte chain. Usually, the larger difference implies the surfactant tends to be vertical to the polyelectrolyte chain, while the small one indicates that the surfactant is apt to be parallel to the polymer, which is

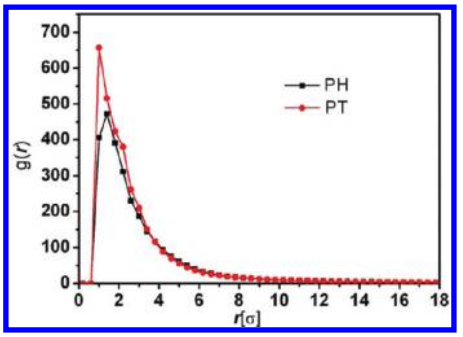

Figure 8. Radial distribution function of the headgroup of the surfactant and the last bead of the surfactant tail around the monomers of the hydrophobic polyelectrolyte at charge ratio $Z = 0.3$.

reaffirmed by the snapshot of the complex in Figure 9. Hence, the surfactant adsorbed on the hydrophobic polyelectrolyte is

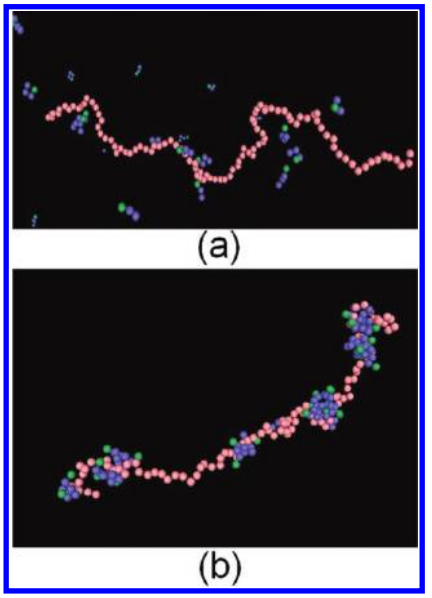

Figure 9. Snapshots of complexes formed by surfactants with hydrophilic polyelectrolyte (a) and hydrophobic polyelectrolyte (b) at $Z = 0.3$.

parallel to the polymer chain than that adsorbed on the hydrophilic one. Furthermore, the morphologies of the complex of surfactant with hydrophilic and hydrophobic polyelectrolyte are also different. Take $Z = 0.3$ as an example; the hydrophobic polyelectrolyte and the surfactant form a necklace structure, which indicates that the surfactant concentration has reached the CAC. However, only the complex with bottle-brush structure is obtained for the system containing hydrophilic polyelectrolyte, which indicates that the current C_{surf} is lower than CAC. The simulation results show that the CAC of surfactant/hydrophobic polyelectrolyte mixed solution is lower than that of the system containing surfactant and hydrophilic polyelectrolyte. The reason should be attributed to the existence of the hydrophobic attractive interaction in addition to the electrostatic interaction between the surfactant and hydrophobic polyelectrolyte. Chu and Thomas[7] have studied the interaction between CTAB and NaPSS, NaPVS, and NaPAA, which have the same linear charge density; they found that the CAC of the surfactant followed the order NaPSS < NaPVS < NaPAA, among which the NaPSS is

dx.doi.org/10.1021/jp212089d | J. Phys. Chem. B 2012, 116, 5516–5526

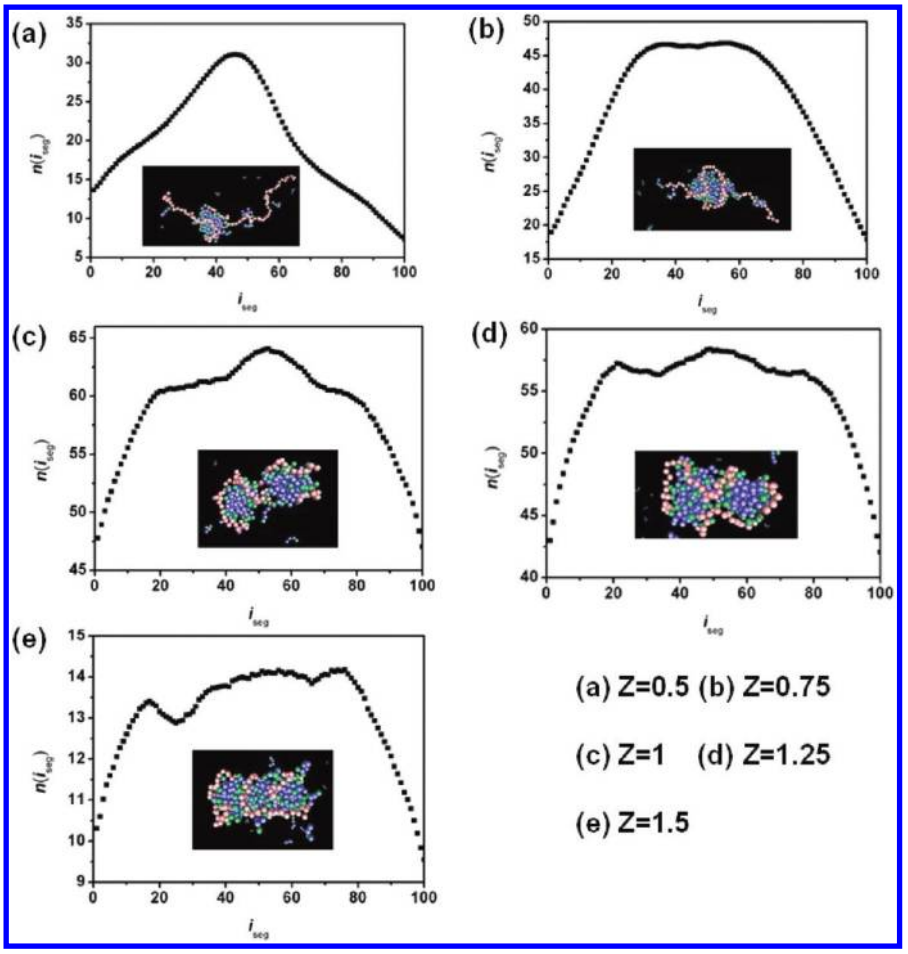

Figure 10. Snapshots of complexes formed by surfactants and hydrophilic polyelectrolyte and the corresponding distribution of surfactant headgroups along the polyelectrolyte chain with different charge ratio Z.

the most hydrophobic. The benzene ring in these polyelectrolytes directly participates in the formation of the micelle, which is in agreement with our results.

3.3. Surfactant Distribution along the Polyelectrolyte Chain. The distribution of the surfactant headroups along the polyelectrolyte chain was quantitatively studied by accounting for the number of surfactant headroups within the distance of $R = 10\sigma$ to a certain bead of the polyelectrolyte. The morphologies of complexes of the surfactant/hydrophilic polyelectrolyte and the distribution of surfactant headgroup on polyelectrolyte at different Z are shown in Figure 10. The surfactant is most likely located on the middle part of the polyelectrolyte chain for $Z = 0.5$. The same result was observed when Linse and Jonsson studied the interaction of macroions and the polyelectrolyte through MC simulation, where the macroions can be taken as more coarse-grained micelles.[37] Limbach et al. studied the distribution of counterions of the strong polyelectrolyte by using MD simulation, and they found that the counterions show a U type distribution along the polymer due to the tail-end effect, which means the counterions prefer to adsorb at the tips of the polymer.[53] Hence, the tail-end effect leads to a strong ionization for the middle of the polymer, where the oppositely charged surfactants are easier to be bind.

With increasing Z, the distribution of surfactant along the polyelectrolyte chain becomes broader. When at $Z = 0.75$, a plateau appears from the 30th to 70th bead of the polyelectrolyte chain, within which the possibility of the surfactant distribution is almost the same. The surfactants absorbed on the polyelectrolyte further aggregate and form a bigger complex. When Z reaches 1.0, the polyelectrolyte adsorbs more surfactants, and multiple hydrophobic areas are formed. Meanwhile, more surfactants enter into the hydrophobic areas due to the hydrophobic interaction, and thus spherical micelles are formed. In the present simulation system, the spherical micelles appear at the two tips of the polyelectrolyte. Yet the amount of the surfactants contained in the two micelles linked by the polyelectrolyte chain is not large enough to neutralize the polyelectrolyte. Consequently, the two mixed micelles carried similar electric charges and will repel each other when they get closer. The structure of the complex can also be detected from the distribution of the surfactant headgroups. It must be pointed out that the cutoff distance we took is larger, so all of the surfactants in the micelle are summed, leading to the appearance of a peak at the middle of the polyelectrolyte chain. Further increasing Z to 1.25, the aggregation number of micelles lying on the polyelectrolyte tips increases, but is still less than 100, and hence no charge inversion was observed for the complex. That is to say, the mixed micelles are still carried with similar charges, although the net charges of the mixed micelles decrease with the increase of aggregation number gradually. However, the depressed net charges do provide the chance for the mixed micelles to be close to each other. From the distribution of the surfactant

dx.doi.org/10.1021/jp212089d | J. Phys. Chem. B 2012, 116, 5516–5526

headgroup, we can see that the peak is smaller than that at Z = 1. The reason for this may be attributed to the dispersion of the surfactant headgroups in the two neighboring micelles derived from the rearrangement of the micelles when they get closer. Increasing Z to 1.5, the peak at the middle of the polyelectrolyte chain totally disappeared, which means that the two micelles at the ends of the polyelectrolyte integrate into a larger aggregate. The simulation snapshot shows the rod-like structure. The results of Nause et al. have shown that only one micelle per chain appears at lower Z and the micelle number per chain increases up to 2 with the increase of Z; this is in agreement with our simulation results.[23] A thermodynamic model by Hansson that describes structures of polyelectrolyte−surfactant complexes can predict the existence of attraction between micelles that are bound to the same polyelectrolyte coils, which leads to a solution of polyelectrolytes with tightly packed micelles in equilibrium with surfactant-free coils.[31] The model considers only the possibility of spherical micelles. Apparently, packed tightly enough micelles could collapse into a single cylindrical micelle. Also, by reducing the penalty of electrostatically unfavorable cylindrical regions through polyelectrolyte binding, the formation of cylinders is favored over spherical micelles as more surfactant binds. In addition, Linse and Jonsson treat the surfactant micelle as oppsitely charged macroions and simulate the system of polyelectrolyte and macroions using Monte Carlo. They find that in the complex, the macroions are able to come into direct contact with each other despite their mutual electrostatic repulsion.[37] However, no micelle fusion was observed because the micelle is considered as a macroion.

Different from the hydrophilic polyelectrolyte system, the headgroups of the surfactants are not stuck on the hydrophobic polyelectrolyte chain any more. The distribution of the surfactant around a hydrophobic polyelectrolyte chain was studied by analyzing the amount of surfactant; the barycenter of them fall in the range (cutoff distance) of $R_c = 5\sigma$ to a certain bead of the polyelectrolyte. As shown in Figure 11, the amount

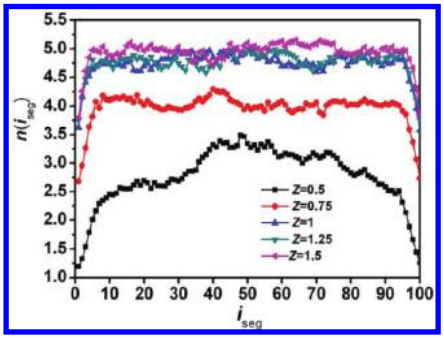

Figure 11. The distribution of the surfactants along the hydrophobic polyelectrolyte chain with different charge ratio Z.

of the surfactant around each bead increases when Z increases from 0.5 to 1. When Z increases from 1 to 1.5, no obvious changes are observed, indicating that the polyelectrolyte has been saturated by surfactants under these conditions. This flatters the results of mean square radius of gyration that will be discussed in the following section: after the saturation, the conformation of the polyelectrolyte chain barely changes. As compared to Figure 10, it can be seen that the distribution of surfactants along the hydrophobic polyelectrolyte chain is more even and dispersed than along the hydrophilic polyelectrolyte chain, and the distribution becomes more even and dispersed with increasing Z.

3.4. Conformational Change of Polyelectrolyte Chain.

The snapshots of the surfactant/polyelectrolyte complexes have shown that the conformation of polyelectrolyte chain undergoes significant changes during the formation of complexes. To obtain more detail information about the conformational change of a polyelectrolyte chain, we further account for the mean square radius of gyration of the polyelectrolyte chain at different Z values. Figure 12 shows the variations of the mean

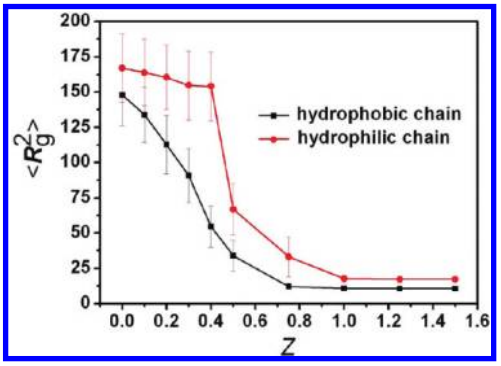

Figure 12. Mean square radius of gyration $\langle R_g^2 \rangle$ of polyelectrolyte versus charge ratio Z.

square radius of gyration for hydrophilic and hydrophobic polyelectrolytes with charge ratio Z. For the hydrophilic polyelectrolyte chain, it can be seen that the change of the mean square radius of gyration of the polyelectrolyte chain is less obvious when increasing Z from 0.1 to 0.4 and the polyelectrolyte is in an extended state. The addition of a small amount of surfactants cannot reduce the repulsion between charged segments in polyelectrolyte effectively; the polyelectrolyte is in the initial state. Upon increasing the number of surfactant molecules bound to polyelectrolyte Z to 0.5, the mean square radius of gyration of the polyelectrolyte is abruptly decreased, which indicates that the concentration of surfactant reached the CAC and the polyelectrolyte becomes curly. The repulsion between charged segments in polyelectrolyte is significantly reduced after introducing more surfactants to the system, which causes the collapse of polyelectrolyte chain. Further increasing Z, the mean square radius of gyration of polyelectrolyte chain continues to reduce until Z = 1, at which the net charge of the polyelectrolyte/surfactants complex is close to zero and the polyelectrolyte chain is saturated by surfactants. After that, the conformation of the polyelectrolyte remains unchanged and independent of Z. Correspondingly, the mean square radius of gyration of polyelectrolyte chain remains constant.

Under the same condition, the hydrophobic polyelectrolyte chain is easier to collapse than the hydrophilic polyelectrolyte chain because the existence of the hydrophobic attractive interaction against the electrostatic repulsion in some degree makes the hydrophobic polyelectrolyte tend to shrink. After the addition of the surfactants, the synergistic effect of the electrostatic attraction between the polyelectrolyte and the surfactant head groups and the hydrophobic interaction between surfactant tails and polyelectrolyte chain promotes more surfactants to bind on the polyelectrolyte chain. The charges carried by polyelectrolyte are shielded effectively by the negatively charged surfactant head groups, leading to the

dx.doi.org/10.1021/jp212089d | J. Phys. Chem. B 2012, 116, 5516−5526

reduction of the repulsion between charged segments in polyelectrolyte. Both the hydrophobic effect of polyelectrolyte chain and the weakened repulsion between charged segments in polyelectrolyte cause the hydrophobic polyelectrolyte chain to collapse rapidly.

Different from the continuous conformational change of the hydrophobic polyelectrolyte, the conformation of the hydrophilic polyelectrolyte chain undergoes a sudden change with increasing Z, which favors the determination of the CAC of the surfactants in hydrophilic polyelectrolyte system by counting the mean square radius of gyration of a polyelectrolyte chain. In the present work, the CAC of the surfactant in the system containing a hydrophilic polyelectrolyte is between the concentrations where Z is in the range of 0.4−0.5, which is consistent with the CAC determined by RDF between surfactant head groups and polyelectrolyte.

It is obviously that there are electrostatic and volume repulsions between the segments for the hydrophilic polyelectrolyte system. When Z is small, polyelectrolyte and surfactants form a bottle-brush structure; hence, the electrostatic interaction between the segments is shielded by the oppositely charged surfactants, which endows the flexibility to the polyelectrolyte chain. However, for the case of a small amount of surfactants adsorbed, the long distance between the adsorbed surfactants prohibits the surfactants from aggregating through hydrophobic interaction. So at this stage the polyelectrolyte remains in the extended state. As a result, although Z increases, the reduction of mean square radius of gyration is not obvious. Once Z reaches a certain value, the tails of surfactants start to aggregate and pull the polyelectrolyte chain, collapsing into the hydrophobic center abruptly. However, for the hydrophobic polyelectrolyte, there is a hydrophobic interaction between each segment besides the electrostatic interaction. When Z is relatively small, they also form the bottle-brush structure at equilibrium state. So as in the hydrophilic polyelectrolyte system, the electrostatic interaction between each segments is weakened due to the adsorptions of the opposite charge surfactants, combined with the hydrophobic interaction between the segments, and so the polyelectrolyte is not so extended. Besides, the hydrophobic interaction between the tails of the surfactant and the polyelectrolyte also leads to the aggregation of the polyelectrolyte segments. Correspondingly, the hydrophobic polyelectrolyte collapses at a relative small Z, and the hydrophobic polyelectrolyte collapses successively with the increase of Z.

3.5. Effect of Charge Density of Polyelectrolyte Chain.

Long-range electrostatic interaction plays an important role in the interaction between oppositely charged surfactant and polyelectrolyte, and the charge density of polyelectrolyte will affect the interaction significantly. The effect of the charge density of polyelectrolyte on the interaction of surfactant and polyelectrolyte was explored in this section. The results have shown that the bottle-brush structure appears at Z = 1.5 (the corresponding system concentration of surfactant $\rho_s\sigma^3 = 7.5 \times 10^{-5}$), and the charge density is −0.5, for the hydrophilic polyelectrolyte system. The necklace structure is not observed until Z reaches 1.5, at which the CAC of the surfactant is reached. Obviously the CAC of the system with lower charge density (−0.5) is much larger than that of the system with higher charge density (−1). It can be seen that the interaction of the surfactant and polyelectrolyte is stronger when the charge density of polyelectrolyte is relatively high. The fact has also been confirmed by Hannsson and Almgren when they studied the interaction between C_nTAB and NaPAA.[17] The main driving force of the interaction between polyelectrolyte and surfactant is the electrostatic attractive interaction when the polyelectrolyte chain is hydrophilic. The increase of the polyelectrolyte charge density enhances the electrostatic attraction between polyelectrolyte and surfactant, which promotes the aggregation of surfactant molecules around the polyelectrolyte chain. It is just the surfactant aggregation that provides the necessary condition for the formation of "necklace". On the contrary, when the polyelectrolyte charge density is low, the attraction between surfactant and polyelectrolyte is relatively weak. The surfactant molecules stroll randomly in the bulk phase, and the chance of approaching polyelectrolyte is deprived partly. At the same time, the electrostatic attraction interaction between the polyelectrolyte and surfactants cannot compensate for the separation effect coming from thermal motion of the molecules. As a result, the formation of the "necklace" is put off until the surfactant concentration is high enough.

We studied the variation of the number of surfactants adsorbed on hydrophilic polyelectrolyte with different charge densities with the total number of the surfactants in the system. Figure 13 shows the charge ratio Z_c of the complex (the ratio of the charge number of surfactants adsorbed on the polyelectrolyte to that carried by the polyelectrolyte) as a function of Z. It can be seen that Z_c depends much on the charge density of polyelectrolyte when Z remains constant, which indicates that the electrostatic interaction dominates the interaction between surfactant and polyelectrolyte. The synergistic effect of the electrostatic interaction between surfactant and polyelectrolyte, and the hydrophobic interaction among the adsorbed surfactants, only can be seen under the condition of the relatively high charge density of the polyelectrolyte chain (such as −1.0) and a large enough amount of adsorbed surfactant. The synergistic effect of electrostatic interaction and hydrophobic interaction leads to a rapid increase of adsorption amount, which is consistent with that discussed in the section of the conformational change of polyelectrolyte chain during surfactant adsorption. However, the synergistic effect is almost negligible when the charge density of polyelectrolyte is low. The limited amount and the far distance of the surfactants bound on the polyelectrolyte with lower charge density lead to the absence of hydrophobic interaction among surfactants.

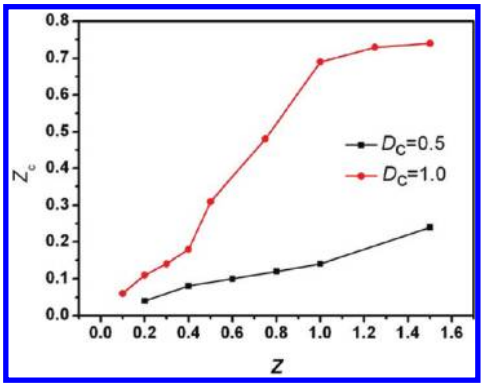

Figure 13. The charge ratio of complex Z_c as a function of that of the system Z with the charge density of the hydrophilic polyelectrolyte D_c = 0.5 and D_c = 1.0.

For the hydrophobic polyelectrolyte system, the charge ratio of the complex Z_c was also studied as a function of Z in the

dx.doi.org/10.1021/jp212089d | J. Phys. Chem. B 2012, 116, 5516−5526

system with various charge density of the polyelectrolyte (the charge density of the polyelectrolyte is −0.5, −0.75, −1.0, and −1.25, respectively), which is shown in Figure 14. As compared

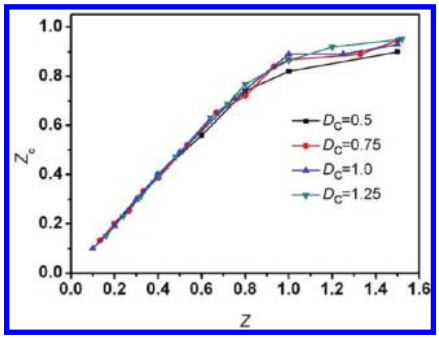

Figure 14. The charge ratio of complex Z_c as a function of Z in the system with various charge density of the hydrophobic polyelectrolyte (the charge density of the polyelectrolyte is −0.5, −0.75, −1.0, and −1.25, respectively).

to the hydrophilic polyelectrolyte, the hydrophobic polyelectrolyte show a different adsorption behavior, where the adsorption amount of the surfactants has a linear relationship with the amount of surfactants in the system before the saturation of the adsorption regardless of the polyelectrolyte charge density. This means that the hydrophobic interaction between surfactant and polyelectrolyte is dominant in the adsorption process for the surfactant/hydrophobic polyelectrolyte system and no synergistic effect is detected under this condition. The electrostatic interaction only determines the adsorption capacity of the polyelectrolyte, which is the absolute amount of the adsorbed surfactants. The results appeal to the continuity of mean square radius of gyration of the polyelectrolyte chain too.

4. CONCLUSIONS

In this work, the interaction between polyelectrolyte and oppositely charged surfactants was investigated by using coarse-grained molecular dynamics simulations. The process of the formation and the morphologies of surfactant/polyelectrolyte complexes were mimicked. The results have shown that the process of surfactants binding on the polyelectrolyte chain can be summarized into four stages. First, surfactants bind on the polyelectrolyte chain and form a "bottle-brush" structure; second, the "bottle-brush" structure evolves into necklace structure; third, the size of the "beads" on the polyelectrolyte chain become gradually larger; and, finally, the polyelectrolyte chain and surfactants form a stable complex micelle. The charge ratio Z of surfactant to polyelectrolyte and the hydrophilicity/hydrophobicity of the polyelectrolyte chain have important effects on the morphology of the complex. The polyelectrolyte chain shows an extended state at low Z, and the bottle-brush structure appears. For the hydrophilic polyelectrolyte system, the surfactant head groups are bound on the polyelectrolyte, while their tails tend to point to the bulk solution. For the hydrophobic polyelectrolyte system, the tails of the surfactants are closer to polyelectrolyte chain. With the increase of Z, the complex micelle is formed accompanying the collapse of the polyelectrolyte chain. For the hydrophilic polyelectrolyte system with intermediate Z, a spherical micelle is formed. Continue to increase Z, and two spherical micelles occur on the polyelectrolyte. With largest Z, two spherical micelles combine into one rod-like micelle. However, for the hydrophobic polyelectrolyte system with the increase Z, only a spherical complex is observed. The collapse mode is different for the two types of polyelectrolyte, too. For the hydrophobic polyelectrolyte chain, the collapse process is continuous, while for the hydrophilic polyelectrolyte chain, it goes through a plateau first and then undergoes a sudden collapse. The effect of charge density of polyelectrolyte on the change of the charge ratio Z_c with that of the system Z is remarkable, but it is different for different polyelectrolyte chains. For the system containing hydrophilic polyelectrolyte, the electrostatic attractive interaction plays a dominant role during the course of surfactant binding on polyelectrolyte. The strong synergistic effect of the electrostatic effect between surfactant and polyelectrolyte, and hydrophobic interaction among the adsorbed surfactants, can be seen when the charge density of the polyelectrolyte chain is relatively high. However, the synergistic effect is almost negligible when the charge density of polyelectrolyte is low. As for the hydrophobic polyelectrolyte system, the electrostatic interaction determines the adsorption capacity of the polyelectrolyte, and the charge density has little effect on the change of Z_c with Z. The hydrophobic interaction plays a dominant role, and no synergistic effect derived form hydrophobic interaction among the adsorbed surfactants is observed during the whole binding process.

■ ASSOCIATED CONTENT

Supporting Information

Snapshot of the transformation of the spherically collapsed structure to a cylindrical shape. This material is available free of charge via the Internet at http://pubs.acs.org.

■ AUTHOR INFORMATION

Corresponding Author

*Tel.: 86-21-64251942. E-mail: shangyazhuo@ecust.edu.cn.

Notes

The authors declare no competing financial interest.

■ ACKNOWLEDGMENTS

This work is supported by the National Natural Science Foundation of China (project nos. 21173079, 21136004), the 111 Project of the Ministry of Education of China (no. B08021), and the Fundamental Research Funds for the Central Universities.

■ REFERENCES

(1) *Interactions of Surfactants with Polymers and Proteins*; Goddard, E. D., Ananthapadmanabahn, K. P., Eds.; CPC Press: Boca Raton, FL, 1993.
(2) *Polymer-Surfactant Systems*; Kwak, J. C. T., Ed.; Surfactant Science Series 77; Marcel Dekker: New York, 1998.
(3) Piculell, L.; Lindman, B. *Adv. Colloid Interface Sci.* **1992**, *41*, 149–178.
(4) Langevin, D. *Adv. Colloid Interface Sci.* **2009**, *147–148*, 170.
(5) Zhou, S. Q.; Chu, B. *Adv. Mater.* **2000**, *12*, 545–556.
(6) Cooper, C. L.; Dubin, P. L.; Kayitmazer, A. B.; Turksen, S. *Curr. Opin. Colloid Interface Sci.* **2005**, *10*, 52–78.
(7) Chu, D. Y.; Thomas, J. K. *Polym. Prepr.* **1986**, *27*, 329–330.
(8) Morishima, Y.; Mizusaki, M.; Yoshida, K.; Dubin, P. L. *Colloids Surf., A* **1999**, *147*, 149–159.
(9) Kosmella, S.; Kötz, J.; Shirahama, K.; Liu, J. *J. Phys. Chem. B* **1998**, *102*, 6459–6464.
(10) Wang, C.; Tam, K. C. *J. Phys. Chem. B* **2004**, *108*, 8976–8982.
(11) Dubin, P. L.; Oeri, R. *J. Colloid Interface Sci.* **1983**, *95*, 453–461.

(12) Almgren, M.; Hansson, P.; Mukhtar, E.; Stam, J. V. *Langmuir* **1992**, *8*, 2405−2412.
(13) Yan, P.; Jin, C.; Wang, C.; Ye, J.; Xiao, J. *J. Colloid Interface Sci.* **2005**, *282*, 188−192.
(14) Hayakawa, K.; Kwak, J. C. T. *J. Phys. Chem.* **1982**, *86*, 3866−3870.
(15) Hayakawa, K.; Kwak, J. C. T. *J. Phys. Chem.* **1983**, *87*, 506−509.
(16) Malovikova, A.; Hayakawa, K.; Kwak, J. C. T. *J. Phys. Chem.* **1984**, *88*, 1930−1933.
(17) Hansson, P.; Almgren, M. *J. Phys. Chem.* **1995**, *99*, 16684−16693.
(18) Wang, C.; Tam, K. C. *Langmuir* **2002**, *18*, 6484−6490.
(19) Wang, C.; Tam, K. C.; Jenkins, R. D.; Tan, C. B. *J. Phys. Chem. B* **2003**, *107*, 4667−4675.
(20) Lee, L. T.; Cabane, B. *Macromolecules* **1997**, *30*, 6559−6566.
(21) Lundahl, P.; Greijer, E.; Sandberg, M.; Cardell, S.; Eriksson, K. O. *Biochim. Biophys. Acta* **1986**, *873*, 20−26.
(22) Viet, D. L.; Lynn, M. W. *Langmuir* **2010**, *26*, 10489−10496.
(23) Nause, R. G.; Hoagland, D. A.; Strey, H. H. *Macromolecules* **2008**, *41*, 4012−4019.
(24) Shirahama, K.; Yuasa, H.; Sugimoto, S. B. *Chem. Soc. Jpn.* **1981**, *54*, 375−377.
(25) Gurovitch, E.; Sens, P. *Phys. Rev. Lett.* **1999**, *82*, 339−342.
(26) Diamant, H.; Andelman, D. *Macromolecules* **2000**, *33*, 8050−8061.
(27) Wallin, T.; Linse, P. *Langmuir* **1998**, *14*, 2940−2949.
(28) Kuhn, P. S.; Diehl, A. *Phys. Rev. E* **2007**, *76*, 041807−041812.
(29) Mateescu, E. M.; Jeppesen, C.; Pincus, P. *Europhys. Lett.* **1999**, *46*, 493−498.
(30) Nguyen, T. T.; Shklovskii, B. I. *Physica A* **2001**, *293*, 324−338.
(31) Hansson, P. *Langmuir* **2001**, *17*, 4167−4180.
(32) Kuhn, P. S.; Levin, Y.; Barbosa, M. C. *Macromolecules* **1998**, *31*, 8347−8355.
(33) Netz, R. R.; Joanny, J -F. *Macromolecules* **1999**, *32*, 9026−9040.
(34) Ferber, C.; von Löwen, H. *Faraday Discuss.* **2005**, *128*, 389−405.
(35) Manning, G. S. *J. Chem. Phys.* **1969**, *51*, 924−933.
(36) Manning, G. S. *Q. Rev. Biophys.* **1978**, *11*, 179−246.
(37) Linse, P.; Jonsson, M. *J. Chem. Phys.* **2001**, *115*, 3406.
(38) Wallin, T.; Linse, P. *J. Phys. Chem.* **1996**, *12*, 305−314.
(39) Wallin, T.; Linse, P. *J. Phys. Chem.* **1996**, *100*, 17873−17880.
(40) Wallin, T.; Linse, P. *J. Phys. Chem.* **1997**, *101*, 5506−5513.
(41) Groot, R. D. *J. Chem. Phys.* **2003**, *118*, 11265−11277.
(42) Groot, R. D. *Langmuir* **2000**, *16*, 7493−7502.
(43) Fischer, A.; Houzelle, M. C.; Hubert, P.; Axelos, M. A. V.; Geoffroy-Chapotot, C.; Carre, M. C.; Viriot, M. L. *Langmuir* **1998**, *14*, 4482−4488.
(44) Sinquin, A.; Hubert, P.; Dellacherie, E. *Langmuir* **1993**, *9*, 3334−3337.
(45) Henni, W.; Deyme, M.; Stchakovsky, M.; LeCerf, D.; Picton, L.; Rosilio, V. *J. Colloid Interface Sci.* **2005**, *281*, 316−324.
(46) Nichifor, M.; Lopes, S.; Bastos, M.; Lopes, A. *J. Phys. Chem. B* **2004**, *108*, 16463−16472.
(47) Darden, T.; York, D.; Pedersen, L. *J. Phys. Chem.* **1993**, *98*, 10089.
(48) Ilekti, P.; Martin, T.; Cabane, B.; Piculell, L. *J. Phys. Chem. B* **1999**, *103*, 9831−9840.
(49) Chang, R.; Yethiraj, A. *J. Chem. Phys.* **2001**, *114*, 7688−7699.
(50) Chang, R.; Yethiraj, A. *J. Chem. Phys.* **2003**, *118*, 6634−6647.
(51) Chang, R.; Yethiraj, A. *Macromolecules* **2006**, *39*, 821−828.
(52) Reddy, G.; Yethiraj, A. *J. Chem. Phys.* **2010**, *132*, 74903−74910.
(53) Limbach, H. J.; Holm, C. *J. Chem. Phys.* **2001**, *114*, 9674−9682.